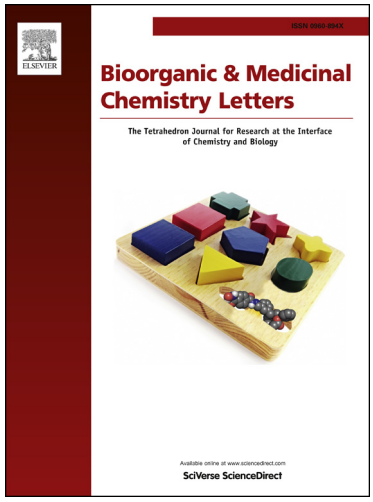

Inhibition of cancer cell invasion by new ((3, 4-dihydroxy benzylidene)hydrazinyl) pyridine-3-sulfonamide analogs

Seong-Mook Kang, Ky-Youb Nam, Seung-Youn Jung, Kyung-Hee Song, Seongho Kho, Kyoung Tai No, Hyun Kyung Choi, Jie-Young Song

PII: S0960-894X(15)30406-6
DOI: http://dx.doi.org/10.1016/j.bmcl.2015.12.093
Reference: BMCL 23454

To appear in: *Bioorganic & Medicinal Chemistry Letters*

Received Date: 7 August 2015
Revised Date: 23 November 2015
Accepted Date: 28 December 2015

Please cite this article as: Kang, S-M., Nam, K-Y., Jung, S-Y., Song, K-H., Kho, S., No, K.T., Choi, H.K., Song, J-Y., Inhibition of cancer cell invasion by new ((3, 4-dihydroxy benzylidene)hydrazinyl) pyridine-3-sulfonamide analogs, *Bioorganic & Medicinal Chemistry Letters* (2015), doi: http://dx.doi.org/10.1016/j.bmcl.2015.12.093

Inhibition of cancer cell invasion by new ((3, 4-dihydroxy benzylidene)hydrazinyl) pyridine-3-sulfonamide analogs

Seong-Mook Kang[a], Ky-Youb Nam[b], Seung-Youn Jung[a], Kyung-Hee Song[a], Seongho Kho[a], Kyoung Tai No[c], Hyun Kyung Choi[d, *], Jie-Young Song[a,*]

[a]Division of Radiation Cancer Research, Korea Institute of Radiological & Medical Sciences, Seoul 139-706, Korea

[b]Center for Development and Commercialization Anti-Cancer Therapeutics, Asan Medical Center, Seoul 138-736, Korea

[c]Department of Biotechnology, Yonsei University, Seoul 120-749, Korea

[d]Department of Medicinal Chemistry, Jungwon University, Goesan, 367-805, Korea

[*]*Corresponding authors. These authors contributed equally to this work. E-mails:* hkchoi45@jwu.ac.kr (H. K. Choi), immu@kirams.re.kr (J.-Y. Song)

Intracellular trafficking plays a key role in eukaryotic cells because it enables shuttling proteins and lipids between cell compartments and thus facilitates constant exchange between organelles.[1, 2] It also mediates many aspects of cell transformation, invasion, and metastasis. Small GTPases of the Rab family, the key regulators of intracellular transport, are involved in the formation of transport carriers from donor membranes, their movement along cytoskelecton tracks, and their fusion with target membranes.[3, 4] The levels of Rab proteins are increased in several human cancers,[2, 5-8] and these GTPases play both an activating and an inhibiting role in tumor progression.[9-13] In their active GTP bound form, Rab GTPases interact with diverse effector proteins in each subcellular location.[14, 15] Among 60 members of the Rab family, Rab27a and Rab27b are present in melanocytes and cytotoxic T lymphocytes, and regulate intracellular transport and exosome secretion in exocrine and endocrine cells.[16, 17] In melanocytes, activated Rab27a localizes to the melanosome membrane, where it acts as a receptor for the actin-dependent motor protein myosin Va; the Rab27–myosin Va interaction is mediated by the melanocyte-specific Rab27a effector melanophilin/Slac2a.[18-20] A loss-of-function mutation in human *RAB27A* gene results in Griscelli syndrome, which is characterized by reduced formation of the tripartite Rab27a–melanophilin–myosin Va complex necessary for actin-dependent melanosome transport; this in turn results in cutaneous albinism and in a loss of cytotoxic activity of T cells.[21, 22] Recent studies have shown that Rab27a is necessary for metastasis and tumor invasion due to its essential role in exosome secretion.[23-26] Wange et al. reported that Rab27a enhances the invasive and metastatic potential of human breast cancer cells by promoting the secretion of insulin-like growth factor-II.[27]

Many researchers have recently focused on targeting vesicle trafficking and exocytosis pathways because blocking exocytosis may permit manipulation of cancer cell behavior and give some clues for development of novel therapeutic strategies. In this regards, an

interesting approach was demonstrated where new blockers of the binding interface between Rab27a and melanophilin were identified by standard pharmacophore-based virtual screening procedures and demonstrated to significantly inhibit melanosome transport.[28] Given the previous finding of Rab27a-targeting hit compound (BMD-11) as shown in Fig. 1, we aim to investigate whether Rab27a inhibition decreases the invasiveness of MDA-MB231 breast cancer cells and A375 malignant melanoma cells. It was found that the di-hydroxyl groups in BMD-11 were critical to hydrogen bond interations in the binding, therefore, we synthesized 15 novel derivatives with di-hydroxyl groups intact but replaced the diethylamine moiety of the BMD-11 with various amine.

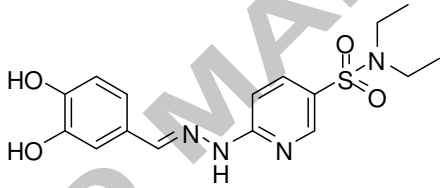

Figure 1. The structure of the BMD-11

Scheme 1 shows preparation of ((3, 4-dihydroxy benzylidene)hydrazinyl)pyridine-3-sulfonamide analogs. Commercial 6-chloropyridine-3-sulfonyl chloride was used as the starting material and 6-chloro sulfonamide compounds (1a–o) with various amines were synthesized.[29] Hydrazinyl sulfonamide compounds (2a–o) were obtained by nucleophilic substitution of analogs 1a–o with hydrazine hydrate.[30] The target dihydroxybenzylidene sulfonamide analogs (3a–o) were synthesized from commercially available 3,4-dihydroxybenzaldehyde in ethanol [31] in very high yields.

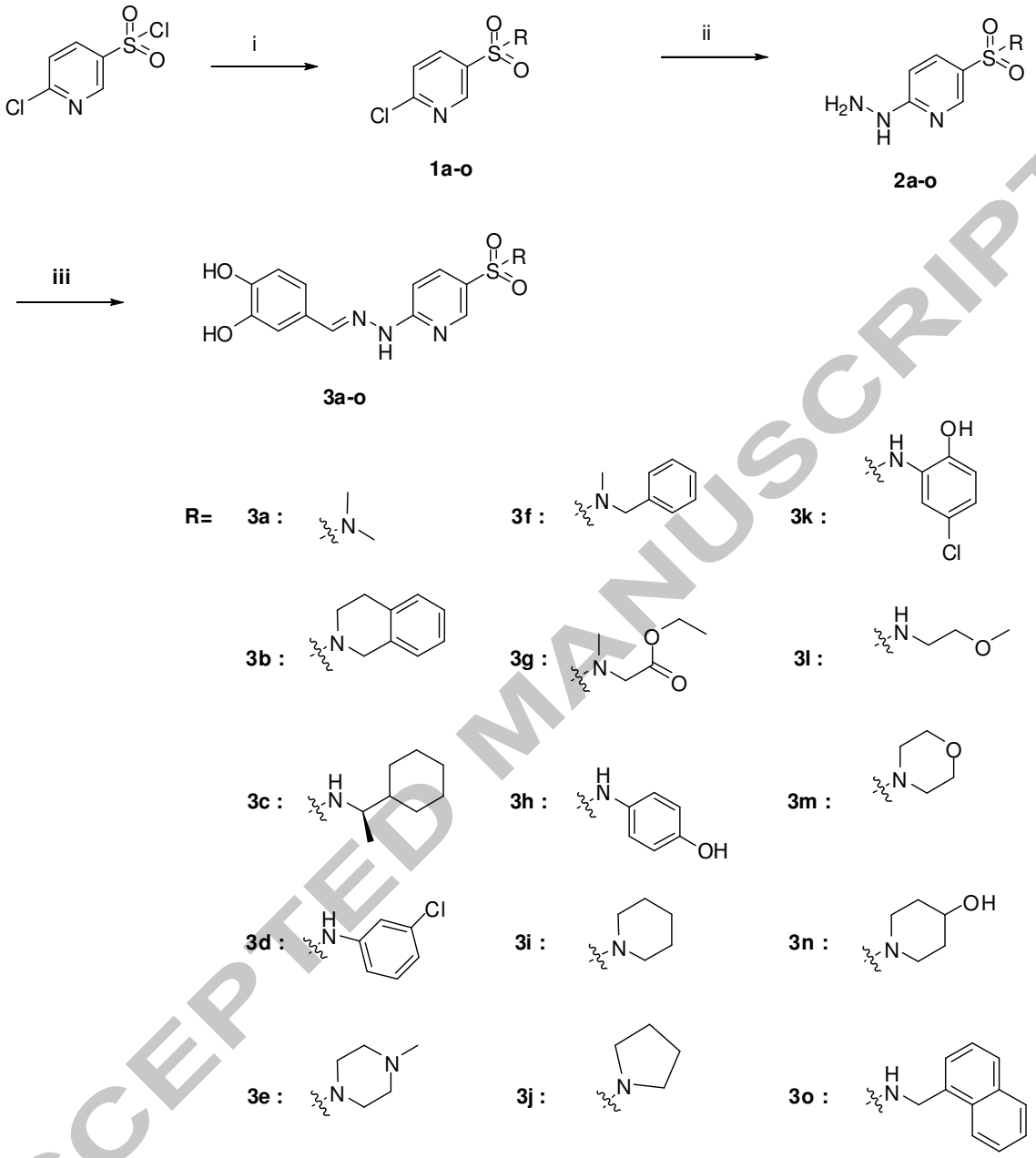

Scheme 1. Reagents and conditions : (i) various amines, chloroform, diisopropylethylamine, ethyl acetate, HCl, r.t.; (ii) hydrazine hydrate, ethanol, 60°C; (iii) 3,4-dihydroxybenzaldehyde, ethanol

Table 1

Structure–activity relationship of sulfonamide analogs.

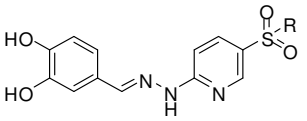

No.	Structure	Cell growth inhibition (% of control at 10 μM)	
	R	**MDA-MB231**	**A375**
Vehicle (DMSO)		0 ± 5.82	0 ± 2.78
3a		4.81 ± 7.09**	1.44 ± 3.17
3b	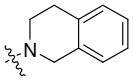	14.87 ± 3.95***	8.41 ± 4.02
3c	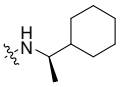	-25.80 ± 4.40	3.45 ± 7.78
3d	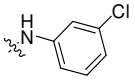	26.34 ± 0.38***	71.66 ± 2.22***
3e	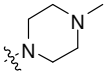	2.10 ± 1.34	1.29 ± 4.36
3f	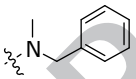	24.62 ± 5.04***	49.39 ± 2.10***
3g	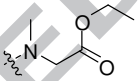	0.97 ± 6.50	-13.68 ± 5.94
3h	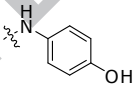	-1.92 ± 5.82	-15.12 ± 3.14
3i		-15.64 ± 11.12	5.06 ± 3.68
3j		-13.56 ± 5.20	-2.01 ± 2.17
3k	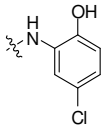	7.47 ± 0.16	-3.03 ± 7.03
3l	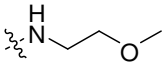	-9.95 ± 5.19	-11.39 ± 6.60
3m	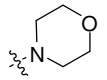	-5.98 ± 6.11	-9.25 ± 7.99
3n	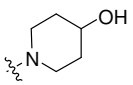	-15.82 ± 8.52	-14.10 ± .678
3o	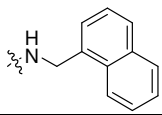	-20.97 ± 6.97	-13.79 ± 6.10

The effect of 15 synthetic compounds (3a–o) on cell viability was evaluated by MTT (3-[4,5-dimethylthiazol-2-yl]-2,5-diphenyltetrazolium bromide) assay in MDA-MB231 and A375 cells (Table 1). MDA-MD231 cells are a representative cell line of triple negative breast cancer, which is clinically aggressive with limited treatment options. The cells were treated with or without each compound (10 μM) for 24 h.

The new analogs, except 3b, 3d, and 3f, showed a tendency for low inhibition activity in cell growth for both cells. Compound 3a, where the diethylamine moiety of BMD-11 was modified into a dimethyl moiety, showed low inhibition value. Compound 3e with piperazine showed somewhat higher inhibition value in both MDA-MB231 and A375 cells when compared with other compounds (3i, 3j, 3m and 3n) containing a heterocyclic moiety. The compound 3d with the aniline moiety inhibited cell growth more efficiently than compounds with a aminophenol moiety (3h and 3k). Compound 3b, 3d and 3f significantly inhibited the growth of MDA-MB231 cells, while 3b only mildly inhibited the growth of A375 cells. However, 3d with chloroaniline and 3f with N-methyl benzyl amine suppressed the growth of A375 cells to a greater extent as compared to that of MDA-MB231 cells.

To differentiate the cytotoxic effect of these compounds from their anti-migratory activity, we next investigated the effect of each compound on the migration of MDA-MB231 cells. As shown in Fig. 2a, compound 3d and 3f markedly blocked wound migration. To quantitatively compare the activity of the synthesized compounds, we determined the density of the cells that migrated inside the scratched areas; the results were represented in Fig. 2b. Insonsistent with the results of cell viability test, compound 3b had not effect on cell migration, but 3i and 3j slightly inhibited migration compared to untreated control cells.

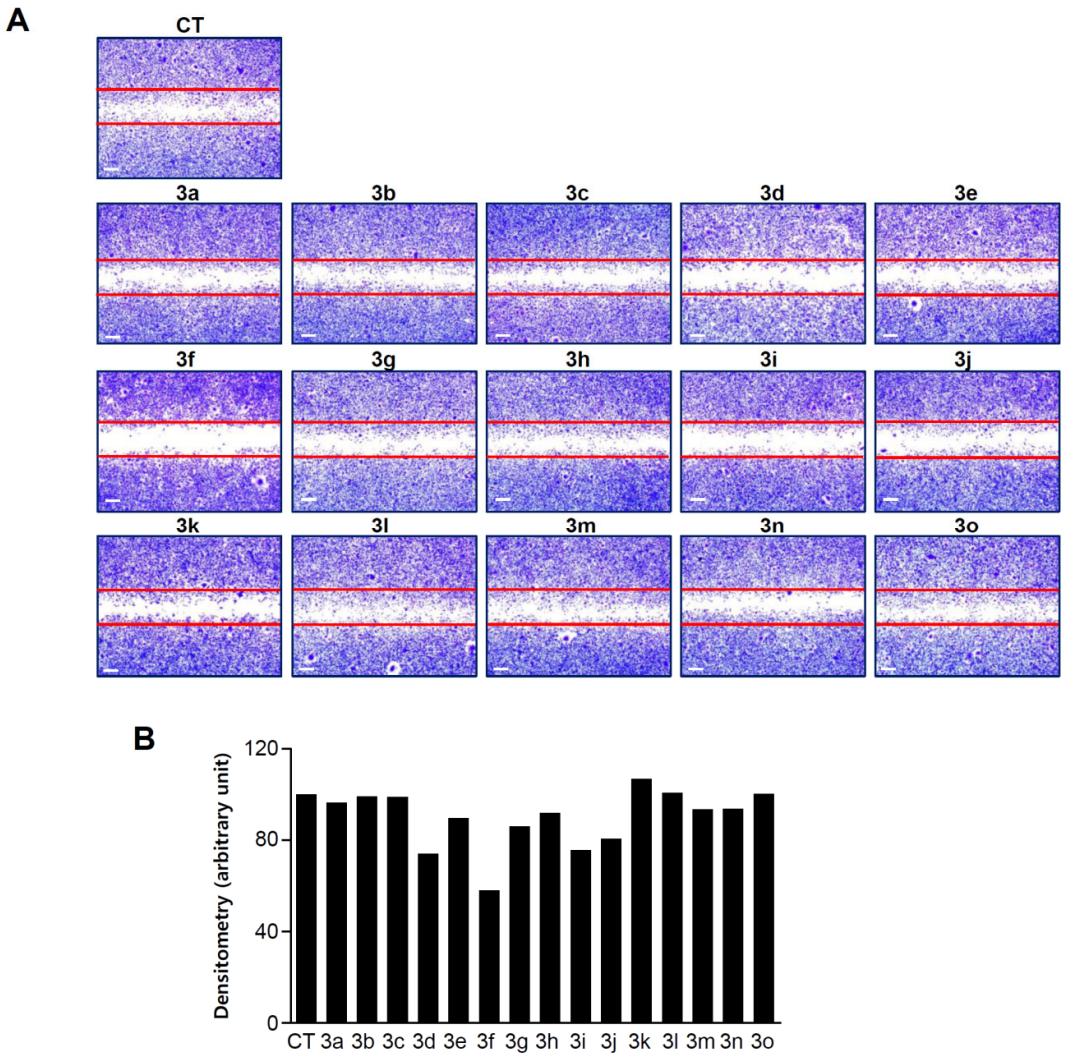

Figure 2. Screening of sulfonamide derivatives (3a–3o) for their effects on breast cancer cell migration. (a) Wound migration assay. (b) Analysis of the anti-migratory effect

To confirm the effect of the 3 compounds (3b, 3d, and 3f) on the migratory and invasive properties of cancer cells, we analysed MDA-MB231 and A375 cells by wound scratch assay and transwell invasion assay in the presence or absence of 3b, 3d, or 3f. Compound 3d significantly inhibited migration and invasion of both cell lines; it also had a cytotoxic effect. Compound 3b had no effect, whereas 3f clearly suppressed migration and invasion of both

cell lines compared to untreated control cells (Fig. 3).

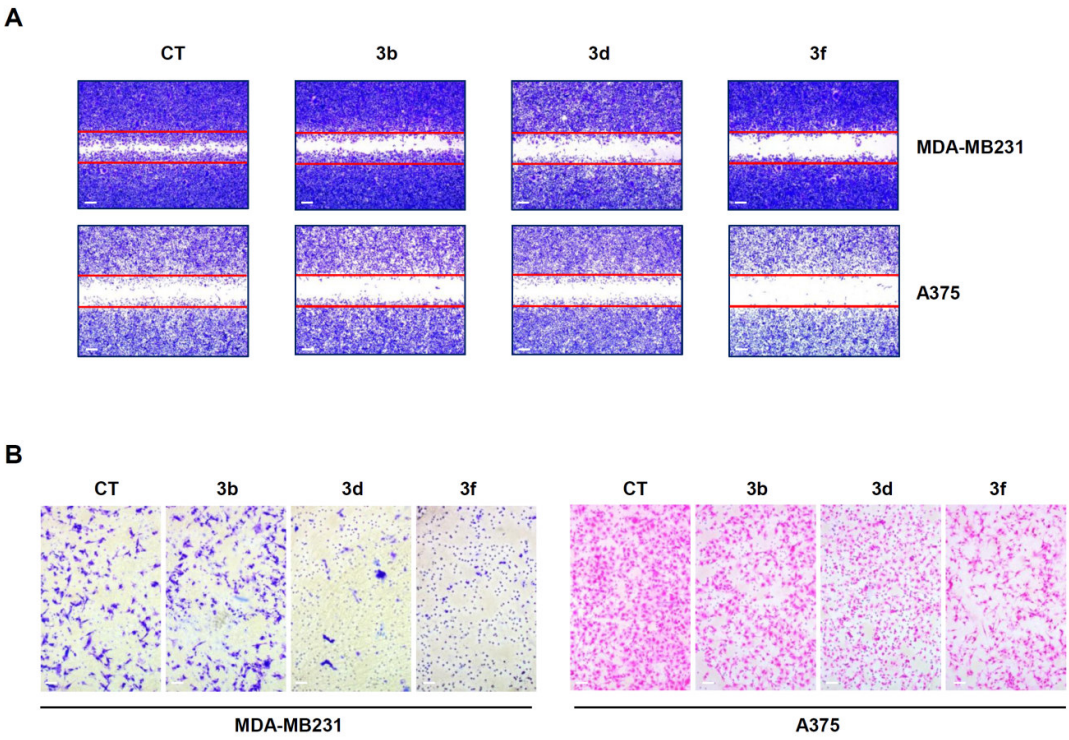

Figure 3. Inhibitory effects of compounds 3b, 3d, and 3f on MDA-MB-231 and A375 cell migration and invasion. (a) Wound scratch assay. (b) Transwell invasion assay

Epithelial–mesenchymal transition (EMT) signaling has been recognized as a key factor affecting cell migration, invasion, and drug resistance in several types of cancer.[32, 33] Therefore, we examined the effect of compounds 3b, 3d, and 3f on the expression of EMT-associated proteins. The levels of representative extracellular matrix (ECM) markers, fibronectin (FN), collagen (Col) and α-smooth muscle actin (α-SMA), were markedly reduced by 3f. Compound 3f significantly reduced the levels of the mesenchymal marker N-cadherin (N-Cad) and vimentin (Vm). Compound 3b had no effect except for a reduction in Vm levels, while 3d considerably inhibited the expression of N-Cad and Vm in both cell lines but did not alter the levels of the ECM markers. The expression of Rab27a was also

attenuated by treatment with 3f and 3d (Fig. 4).

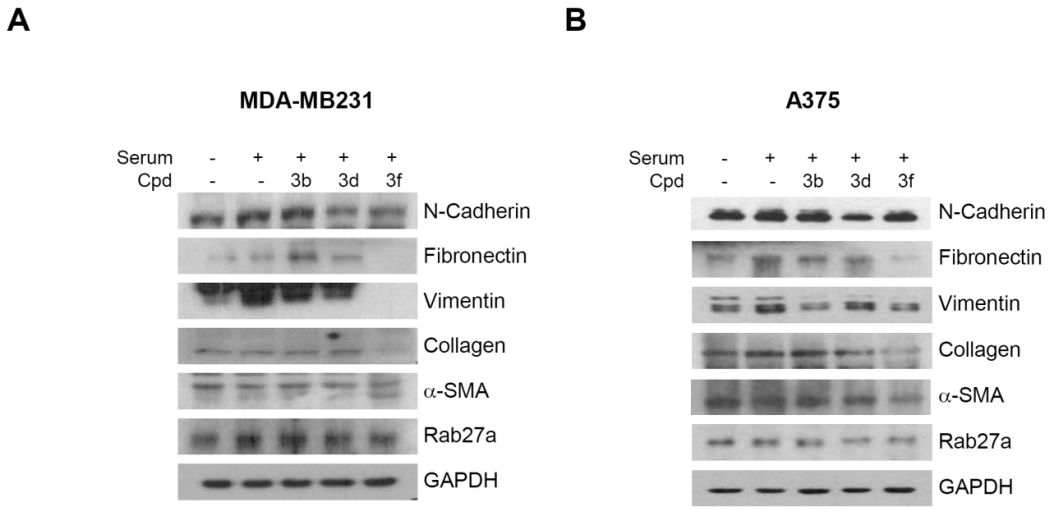

Figure 4. Effects of compounds 3b, 3d, and 3f on the expression of EMT-associated markers. (a) MDA-MB-231 cells. (b) A375 cells

Based on the results of biological evauations, a docking study of selected compounds was performed. The X-ray structure of the Rab27a–Exophilin4/Slp-a complex was used for modeling, which was retrieved from the PDB (PDB ID = 3BC1).[34] The binding interface between Rab27a and Exophilin4 is centered between the residues of an invariant hydrophobic triad (Phe46, Trp73, and Phe88). An extended hydophobic cluster is formed by Ile39, Thr41, and Val42 (Fig. 5a). Asp91 of Rab27a is a key residue for interaction with Slp-a, because an Asp91 mutant is unable to bind Slp-a.[35] The binding site for the tested compounds was formed by four key residues (Phe46, Trp73, Phe88, and Asp91), which interacted with 3f, 3i, and 3o (Fig. 5b). Computations were performed on a Windows platform using DS modeling/CDOCKER (Accelrys Inc., San Diego, USA) with the CHARMM force field.[36] The molecular dynamics (MD) simulated annealing process is performed using a flexible

ligand docking. The final minimization step is applied to ligand's docking pose. The minimization consists of 1,000 steps of steepest descent using an energy tolerance of 0.001 kcal/mol.

Table 2

Relation between biological activity and docking scores of 3f, 3i, and 3o

	3f	3i	3o
Docking score (Ludi score[37])	572	462	489
Docking score (LigScore score[38])	4.01	3.31	3.77
A375 cell growth inhibition (% of control)	49.39	5.06	-13.79

These studies were performed using the LigandFit[39] module as implemented in Discovery Studio 3.0 (Accelrys Inc., San Diego, CA, USA).

The relationship between cell growth inhibition and docking scores is shown in Table 2. Given that the value of Ludi score of 600 usually implies 1.0 μM of enzyme activity,[37] the Ludi score of compound 3f (572) was high. Compound 3f also exhibited the best biological activity. It interacted with Rab27a via hydrophobic interactions between the dihydroxylbenzyl group and the invariant hydrophobic triad of the protein; the dihydroxyl group also formed three strong hydrogen bonds with the side chains of Asp91 and Lys11 (red dotted line in Fig 5c.). Dihydroxyl benzyl groups have been previously described as key players in intermolecular interactions as hydrogen bond donors.[28] Benzyl sulfonamide of 3f also had a weak hydrogen bond (yellow dotted line in Fig. 5c.) and a hydrophobic interaction between the terminal benzyl group and the side chain of Val42. However, 3-hydroxyl group in compound 3i did not form a hydrogen bond with the side chain of Asp91, and did not have a hydrophobic interaction between the piperidin-1-ylsulfonyl group and the side chain of

Val42 (Fig. 5d). The other compounds with terminal hydrophilic functional groups such as ester, hydroxyl, or morpholine (3g, 3h, 3l, and 3m) showed low biological activity. Their terminal hydrophilic functional groups did not interact with the extended hydophobic cluster (the side chain of Val42). We suggest that the three hydrogen bonds between dihydroxyl benzyl groups and side chains of Asp91 and Lys11, and the additional hydrophobic interaction between the terminal sulfonamide functional group and the extened hydrophobic cluster may play a key role in biological activity.

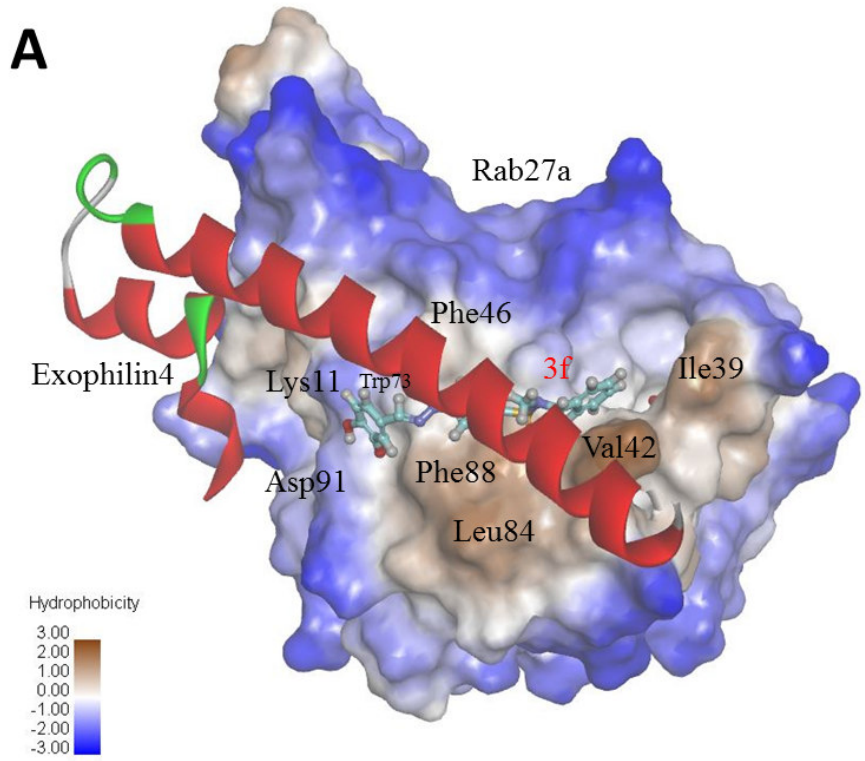

B

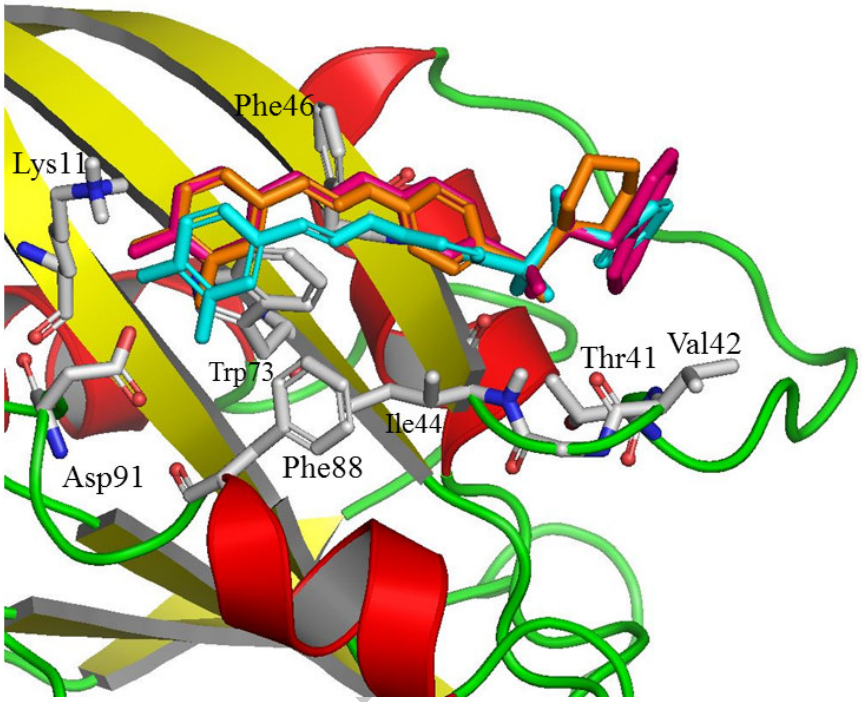
Phe46
Lys11
Trp73
Thr41
Val42
Ile44
Asp91
Phe88

C

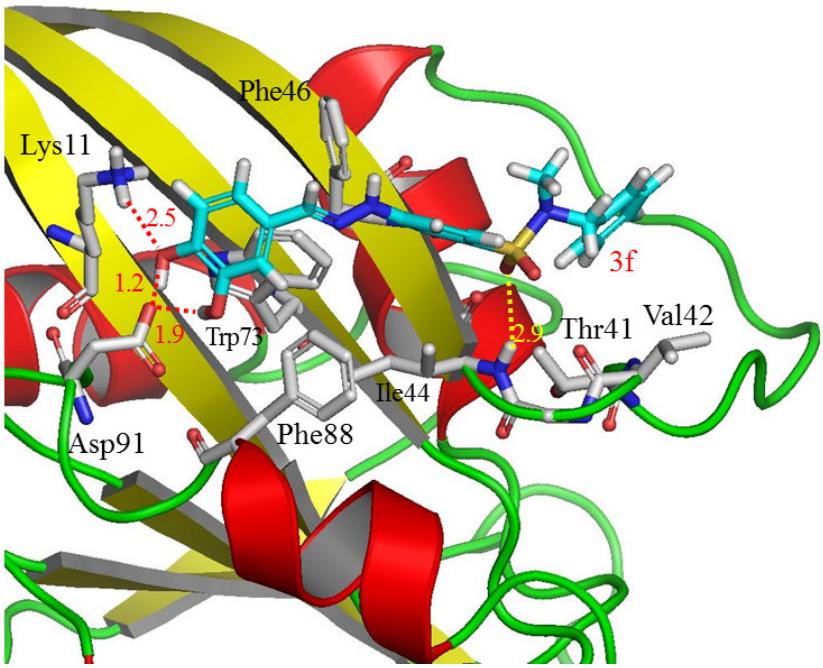
Phe46
Lys11
2.5
1.2
1.9
Trp73
3f
2.9
Thr41
Val42
Ile44
Asp91
Phe88

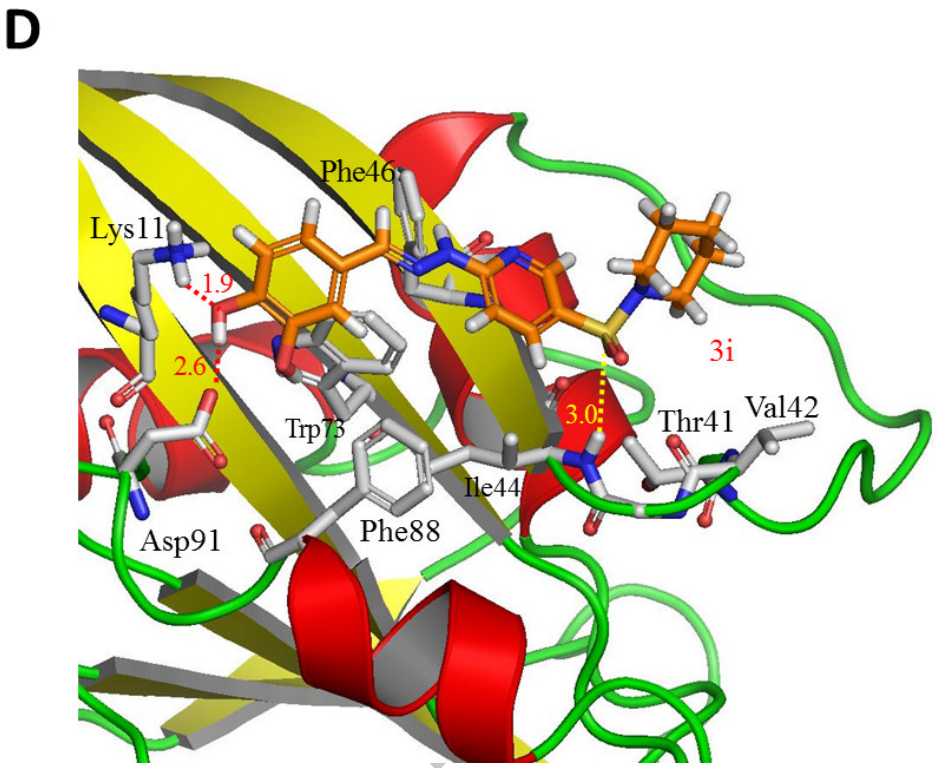

Figure 5. Predicted docking poses of 3,4-dihydroxybenzylidene hydrazinyl pyridine sulfonamide analogs 3f, 3i, and 3o on Rab27a (PDB entry 3BC1). (a) The surface of Rab27a was rendered on the basis of Kyte and Doolittle hydrophobicity and colored using a color gradient from red (hydrophobic amino acids) to blue (hydrophilic amino acids). (b) Superposition of the binding modes of 3f (cyan), 3i (orange), and 3o (magenta) in the binding site of Rab27a. (c) The proposed docking conformation of compound 3f in the binding site of Rab27a. Red and yellow dotted lines indicate hydrogen bonds between compound 3f and the receptor. Key binding residues of the receptor are shown in stick representation (carbon, light gray). (d) Proposed docking conformation of compound 3i in the binding site of Rab27a. The model was generated using Pymol (http://www.pymol.org).

In conclusion, we have developed new compounds, characterized by a N-methyl benzyl sulphonamide functional group, which are able to inhibit cancer cell invasion and metastasis. Compound 3f decreased the expression of signature ECM markers (FN, Col, and α-SMA), and mesenchymal markers (N-Cad, and Vm). Compound 3f also markedly inhibited wound repair and tumor invasion in *in vitro* assays. These findings demonstrate that a new synthetic compound targeting Rab27a could inhibit invasion and metastasis of human breast carcinoma and melanoma cells. Our findings thus may provide a promising approach to decrease recurrence of several solid tumors.

Acknowledgments

This work was supported by the Nuclear R&D Program of the Ministry of Science, ICT and Future planning, Republic of Korea (Grant No. 1711021781).

References and Notes

1. Pereira, M. M.; Santana, M.; Teixeira, M. *Biochim. Biophys. Acta*. **2001**, *1505*, 185.

2. Zerial, M.; McBride, H. *Nat. Rev. Mol. Cell Biol*. **2001**, *2*, 107.

3. Stenmark, H. *Nat. Rev. Mol. Cell Biol*. **2009**, *10*, 513.

4. Yasukawa, Z.; Naito, Y.; Takagi, T.; Mizushima, K.; Tokunaga, M.; Ishihara, N.; L, R. J.; Yoshikawa, T. *J. Clin. Biochem. Nutr*. **2012**, *51*, 33.

5. Burns, M. E.; Sasaki, T.; Takai, Y.; Augustine, G. J. *J. Gen. Physiol.* **1998**, *111*, 243.

6. Ohya, T.; Sasaki, T.; Kato, M.; Takai, Y. *J. Biol. Chem*. **1998**, *273*, 613.

7. Pfeffer, S. R. *Trends Cell Biol.* **2001**, *11*, 487.

8. Seabra, M. C.; Mules, E. H.; Hume, A. N. *Trends Mol. Med*. **2002**, *8*, 23.

9. Fukui, K.; Tamura, S.; Wada, A.; Kamada, Y.; Igura, T.; Kiso, S.; Hayashi, N. *Hepatol. Res.* **2007**, *37*, 957.

10. Hou, Q.; Wu, Y. H.; Grabsch, H.; Zhu, Y.; Leong, S. H.;Ganesan, K.; Cross, D.; Tan, L. K.; Tao, J.; Gopalakrishnan, V.; Tang, B. L.; Kon, O. L.; Tan, P. *Cancer Res.* **2008**, *68*, 4623.

11. Cheng, K. W.; Lahad, J. P.; Kuo, W. L.; Lapuk, A.; Yamada, K.; Auersperg, N.; Liu, J.; Smith-McCune, K.; Lu, K. H.; Fishman, D.; Gray, J. W.; Mills, G. B. *Nat. Med*. **2004**, *10*, 1251.

12. Agarwal, R.; Jurisica, I.; Mills, G. B.; Cheng, K.W. *Traffic* **2009**, *10*, 1561.

13. Goldenring, J. R.; Nam, K. T. *Br. J. Cancer* **2011**, *104*, 33.

14. Cheviet, S.; Coppola, T.; Haynes, L. P.; Burgoyne, R. D.; Regazzi, R. *Mol. Endocrinol.* **2004**, *18*, 117.

15. Jordens, I.; Westbroek, W.; Marsman, M.; Rocha, N.; Mommaas, M.; Huizing, M.; Lambert, J.; Naeyaert, J. M.; Neefjes, *Pigment Cell Res*. **2006**, *19*, 412.

16. Tolmachova, T.; Anders, R.; Stinchcombe, J.; Bossi, G.; Griffiths, G. M.; Huxley, C.; Seabra, M. C. *Mol. Biol. Cell* **2004**, *15*, 332.

17. Izumi, T. *Endocr. J*. **2007**, *54*, 649.

18. Fukuda, M.; Kuroda, T. S. *J. Biol. Chem*. **2002**, *277*, 43096.

19. Strom, M.; Hume, A. N.; Tarafder, A. K.; Barkagianni, E.; Seabra, M. C. *J. Biol. Chem.* **2002**, *277*, 25423.

20. Westbroek, W.; Lambert, J.; Bahadoran, P.; Busca, R.; Herteleer, M. C.; Smit, N.; Mommaas, M.; Ballotti, R.; Naeyaert, J. M. *J. Invest. Dermatol.* **2003**, *120*, 465.

21. Menasche, G.; Pastural, E.; Feldmann, J.; Certain, S.; Ersoy, F.; Dupuis, S.; Wulffraat, N.; Bianchi, D.; Fischer, A.; Le Deist, F.; de Saint Basile, G. *Nat. Genet.* **2000**, *25*, 173.

22. Tolmachova, T.; Ramalho, J. S.; Anant, J. S.; Schultz, R. A.; Huxley, C. M.; Seabra, M. C. *Gene* **1999**, *239*, 109.

23. Li, W.; Mu, D.; Tian, F.; Hu, Y.; Jiang, T.; Han, Y.; Chen, J.; Han, G.; Li, X. *Mol. Med. Rep*. **2013**, *8*, 1876.

24. Bobrie, A.; Krumeich, S.; Reyal, F.; Recchi, C.; Moita, L. F.; Seabra, M. C.; Ostrowski, M.; Thery, C. *Cancer Res*. **2012**, *72*, 4920.

25. Li, W.; Hu, Y.; Jiang, T.; Han, Y.; Han, G.; Chen, J.; Li, X. *APMIS*. **2014**, *122*, 1080.

26. Hendrix, A.; Hume, A. N. *Int. J. Dev. Biol*. **2011**, *55*, 879.

27. Wang, J. S.; Wang, F. B.; Zhang, Q. G.; Shen, Z. Z.; Shao, Z. M. *Mol. Cancer Res*. **2008**, *6*, 372.

28. Joung, J. Y.; Lee, H. Y.; Park, J.; Lee, J. Y.; Chang, B. H.; No, K. T.; Nam, K. Y.; Hwang, J. S. *Appl. Biochem. Biotechnol*. **2014**, *172*, 1882.

29. Nikam, S. S.; Kornberg, B. E.; Ault-Justus, S. E.; Rafferty, M. F. *Tetrahedron Lett*. **1998**, *39*, 1121.

30. Pommery, N.; Taverne, T.; Telliez, A.; Goossens, L.; Charlier, C.; Pommery, J.; Goossens, J. F.; Houssin, R.; Durant, F.; Henichart, J. P. *J. Med. Chem*. **2004**, *47*, 6195.

31. Khan, K. M.; Shah, Z.; Ahmad, V. U.; Khan, M.; Taha, M.; Rahim, F.; Jahan, H.; Perveen, S.; Choudhary, M. I. *Med. Chem*. **2011**, *7*, 572.

32. Larue, L.; Bellacosa, A. *Oncogene* **2005**, *24*, 7443.

33. Heerboth, S.; Housman, G.; Leary, M.; Longacre, M.; Byler, S.; Lapinska, K.; Willbanks, A.; Sarkar, S. *Clin. Transl. Med*. **2015**, *4*, 6.

34. Chavas, L. M.; Ihara, K.; Kawasaki, M.; Torii, S.; Uejima, T.; Kato, R.; Izumi, T.; Wakatsuki, S. *Structure* **2008**, *16*, 1468.

35. Itzen, A.; Goody, R.S. *Structure* **2008**, *16*, 1437.

36. Wu, G.; Robertson, D. H.; Brooks, C. L. 3rd; Vieth, M. *J. Comput. Chem.* **2003**, *24*, 1549.

37. Bohm, H. J. *J. Comput. Aided Mol. Des.* **1998**, *12*, 309.

38. Krammer, A.; Kirchhoff, P. D.; Jiang, X.; Venkatachalam, C. M.; Waldman, M. *J. Mol. Graph. Model* **2005**, *23*, 395.

39. Venkatachalam, C. M.; Jiang, X.; Oldfield, T.; Waldman, M. *J. Mol. Graph. Model* **2003**,

21, 289.

Figure Captions

Figure 1. The structure of the BMD-11

Figure 2. Screening of sulfonamide derivatives (3a–3o) for their effects on breast cancer cell migration. (a) Wound migration assay. (b) Analysis of the anti-migratory effect

Figure 3. Inhibitory effects of compounds 3b, 3d, and 3f on MDA-MB-231 and A375 cell migration and invasion. (a) Wound scratch assay. (b) Transwell invasion assay

Figure 4. Effects of compounds 3b, 3d, and 3f on the expression of EMT-associated markers. (a) MDA-MB-231 cells. (b) A375 cells

Figure 5. Predicted docking poses of 3,4-dihydroxybenzylidene hydrazinyl pyridine sulfonamide analogs 3f, 3i, and 3o on Rab27a (PDB entry 3BC1). (a) The surface of Rab27a was rendered on the basis of Kyte and Doolittle hydrophobicity and colored using a color gradient from red (hydrophobic amino acids) to blue (hydrophilic amino acids). (b) Superposition of the binding modes of 3f (cyan), 3i (orange), and 3o (magenta) in the binding site of Rab27a. (c) The proposed docking conformation of compound 3f in the binding site of Rab27a. Red and yellow dotted lines indicate hydrogen bonds between compound 3f and the receptor. Key binding residues of the receptor are shown in stick representation (carbon, light gray). (d) Proposed docking conformation of compound 3i in the binding site of Rab27a. The model was generated using Pymol (http://www.pymol.org).

Graphical Abstract

To create your abstract, type over the instructions in the template box below.
Fonts or abstract dimensions should not be changed or altered.

Inhibition of cancer cell invasion by new ((3, 4-dihydroxy benzylidene)hydrazinyl) pyridine-3-sulfonamide analogs

Leave this area blank for abstract info.

Seong-Mook Kang, Ky-Youb Nam, Seung-Youn Jung, Kyung-Hee Song, Seongho Kho, Kyoung Tai No, Hyun Kyung Choi*, Jie-Young Song*